

# **Nuclear Data Measurement Activities in China —Progress Report to NEA WP Meeting**

(April 2, 2001)

**Liu Tingjin**

(Chinese Nuclear Data Center)

Nuclear data measurements have been continuously done for last two years at China Institute of Atomic Energy and in Chinese Nuclear Data Network(CNDN), including Peking University (BJG), Sichuan University (SIU), Lanzhou University (LNZ) etc.

## **1. Neutron Double Differential Cross Section (DDX)**

The **DDX of  ${}^9\text{Be}(n,n \text{ emission})$**  at incident neutron energy **5.9 and 6.4 MeV** were measured at Institute of Heavy Ion Physics, Peking University with Van de Grraff accelerator by means of **time-of-flight method**. The neutrons were produced by  $\text{D}(d,n)$  reaction using a deuterium gas target. The secondary neutron detector is a ST-451 liquid scintillator. The time resolution is about 2ns. The flight path is 376.8cm. The measurements were made at 10 angles from  $25^\circ$  and  $150^\circ$ . The results with comparing the data of LANL (5.9 MeV) and Tohoku (6.4 MeV) are shown in Figs.1 and 2. It can be seen that there is higher energy resolution for present data, so that the peaks at the high energy part corresponding to the inelastic scattering to the discrete levels are sharper. But present data are much low than the data of both LANL and Tohoku at low energy part of the spectra.

The **DDX of  $(n,n \text{ emission})$**  at incident neutron energy **10 MeV** were measured at CIAE with Hi-13 Tandem by means of both **normal and abnormal time-of-flight spectrometers**.

The measurements were made at about 7 angles between 35° and 120°. The neutrons were produced by D(d,n) neutron source and the abnormal TOF spectrometer was used to separate the d-d breakup continuous neutron for measuring low energy part of the secondary neutron spectrum. Now the measurements for  $^{6,7}\text{Li}$  have been completed, but the data is still being processed now.

## 2. Activation Cross Section

The excitation functions have been continuously measured by several groups for last two years in China with **activation method**.

The  $^{186}\text{W}$ ,  $^{75}\text{As}$ ,  $^{141}\text{Pr}$ ,  $^{50}\text{Cr}(n,\gamma)$  cross section was measured in the energy range from **0.5 to 1.5 MeV** at **Peking University**. The experiments were performed at 4.5 MV Van de Graaff accelerator of the Institute of Heavy Ion Physics. The monoenergetic neutrons were produced via T(p,n) reaction on a solid T-Ti target. ORTEC HPGe  $\gamma$  detector (105 cm<sup>3</sup>) were used. The results for  $^{186}\text{W}$  are shown in Fig.3.

The cross sections were measured at **Sichuan University** in the energy region from **0.029 to 1.1 MeV** for  $^{75}\text{As}(n,\gamma)$  reaction and from **0.16 to 1.2 MeV** for  $^{174}\text{Hf}(n,\gamma)$  reaction.

The following reaction cross sections were measured at 14.7 MeV at **Lanzhou University**:  $^{52}\text{Cr}(n,2n)^{51}\text{Cr}$ ,  $^{103}\text{Rh}(n,2n)^{102}$ ,  $^{151}\text{Eu}(n,\alpha)^{148g,148m}\text{Pm}$ ,  $^{153}\text{Eu}(n,2n)^{152m}\text{Eu}$ ,  $^{153}\text{Eu}(n,p)^{153}\text{Sm}$ ,  $^{153}\text{Eu}(n,\alpha)^{150}\text{Pm}$ ,  $\text{Rh}^{185}\text{Re}(n,2n)^{185m,184g}\text{Re}$ ,  $^{191}\text{Ir}(n,2n)^{190}\text{Ir}$ .

## 3. Fission Product Yield

The fission product yield has been continuously measured at **CIAE** by means of **direct gamma spectrum method**. The mass distributions from  $^{235,238}\text{U}$  fission at high incident neutron energies **19.1 and 22 MeV** were measured in last two years. HPGe gamma spectrometry was used to measure the activities of fission products.

Absolute fission rate was monitored with a double-fission chamber, which was covered with Cd foil of 1 mm thickness to shield thermal neutron in the environment. Threshold detector method (for 19.1 MeV) and time-of-flight method (for 22.0 MeV) were used to measure the neutron spectra in order to estimate the fission events induced by break-up neutrons and scattering neutrons. The **chain yields** were determined for **39 product nuclides at 19.1 MeV, for 33 product nuclides at 22.0 MeV from  $^{238}\text{U}$  fission; for 35 product nuclides at 19.1 MeV, for 30 product nuclides at 22.0 MeV from  $^{235}\text{U}$  fission.** The results are given in Figs 4-6.

#### **4. Charge Particle Double Differential Cross Section**

The angular distributions and cross sections were measured for  $^{10}\text{B}(\text{n},\alpha)^7\text{Li}$ ,  $^{64}\text{Zn}(\text{n},\alpha)^{61}\text{Ni}$  reactions at **5.0, 5.7 and 6.7 MeV** incident neutron energies at **Peking University**. The experiment was performed at the 4.5 MV Van de Graaff accelerator of the Heavy Ion Physics. Monoenergetic neutrons were produced through D(d,n) reaction with a deuteron gas target. The **gridded ionization chamber** was used to detect the emission charge particles. Absolute neutron flux was determined through  $^{238}\text{U}(\text{n},\text{f})$  reaction. The results are given in Figs. 7-10 for  $^{64}\text{Zn}$  and Figs. 11-15 for  $^{10}\text{B}$ .

#### **5. $\gamma$ Product Data**

The **discrete  $\gamma$  product cross sections** for nuclides  $^{16}\text{O}$ , **Fe, Al and C** were measured at **CIAE** in the energy region from **7.0 to 13 MeV**. The measurements were performed at Hi-13 Tandem by using **time-of-flight method and anti-Compton detector**.

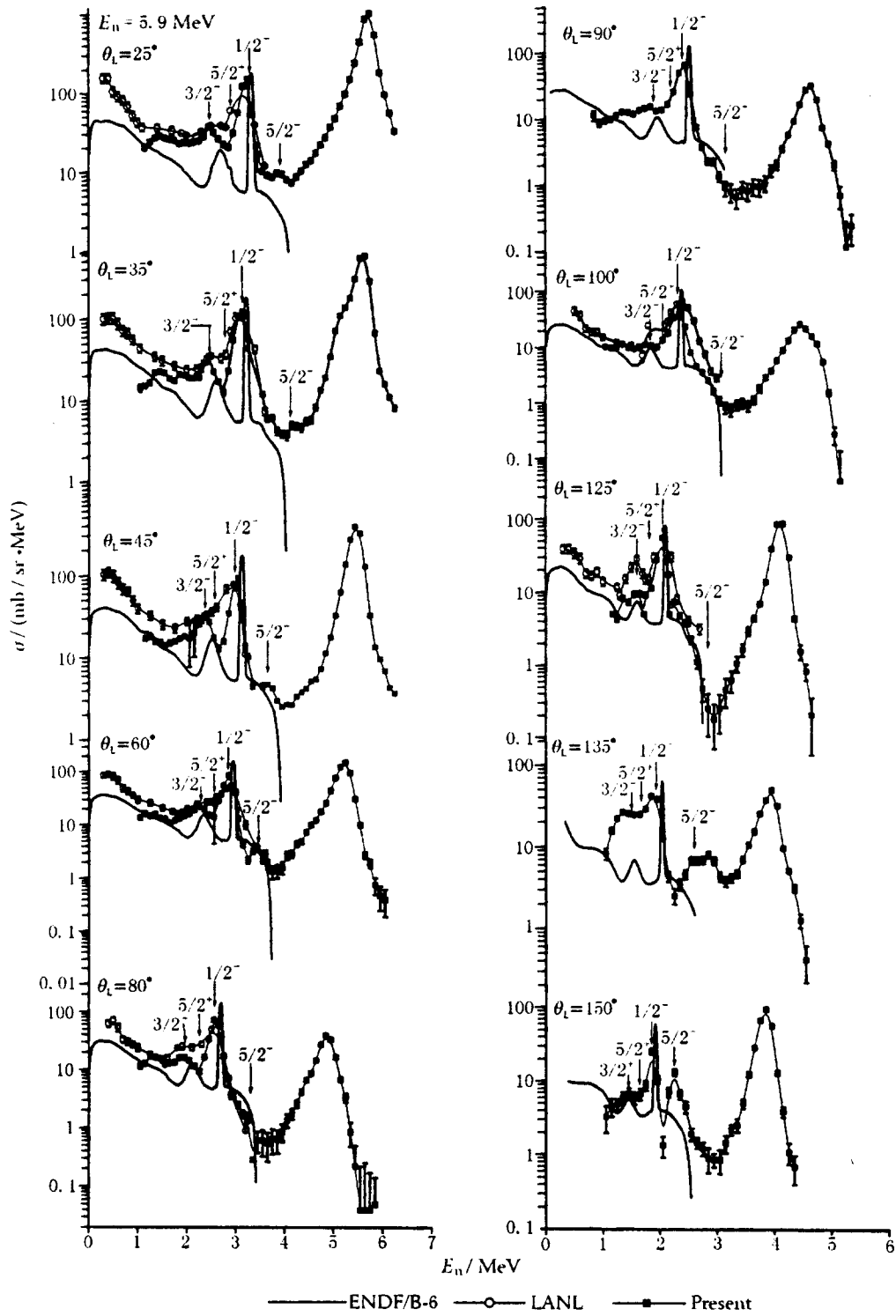


Fig.1 Double differential cross section of  ${}^9\text{Be}$  at 5.9 MeV

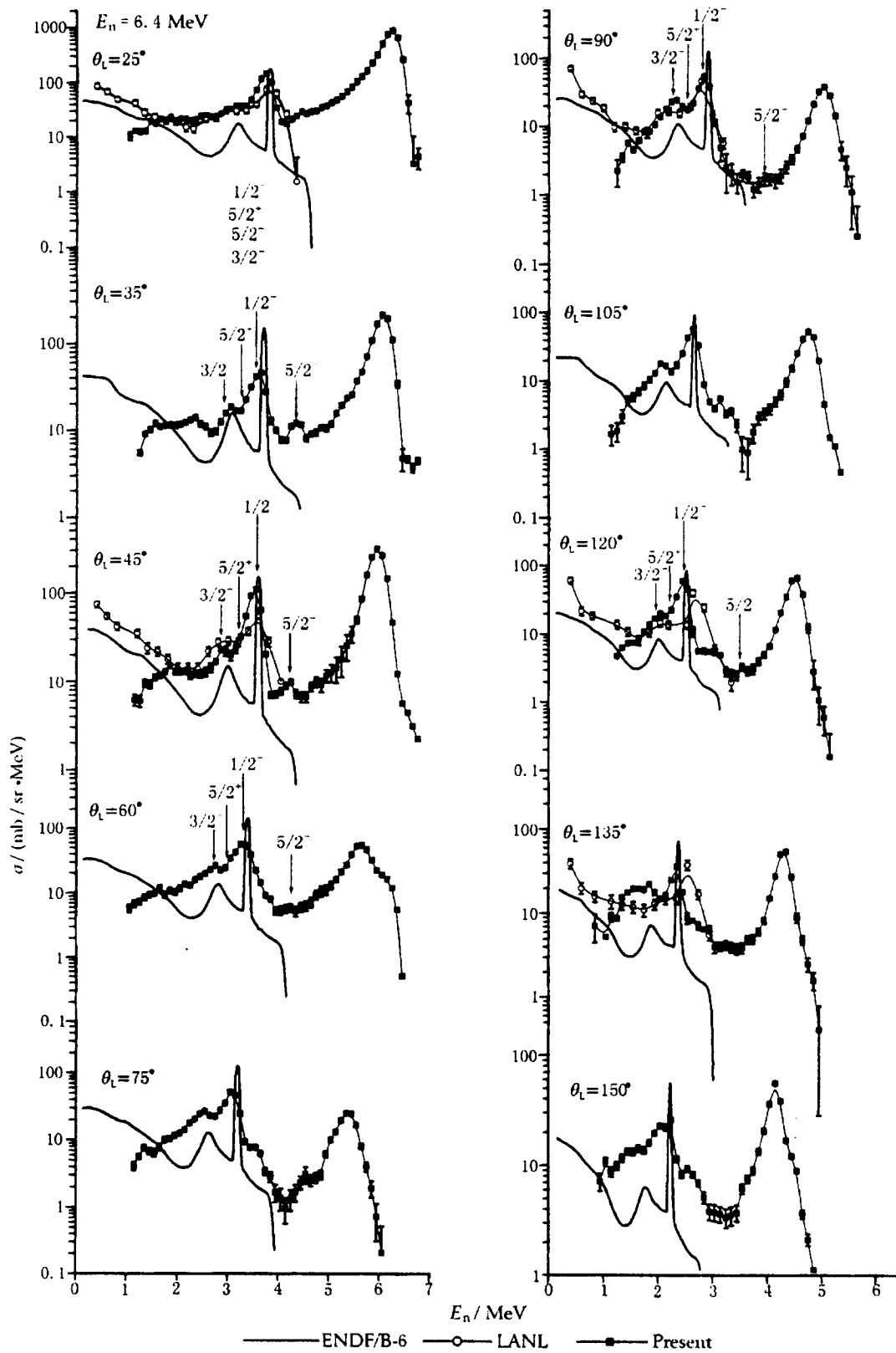


Fig. 2 Double differential cross section of  $^9\text{Be}$  at 6.4 MeV

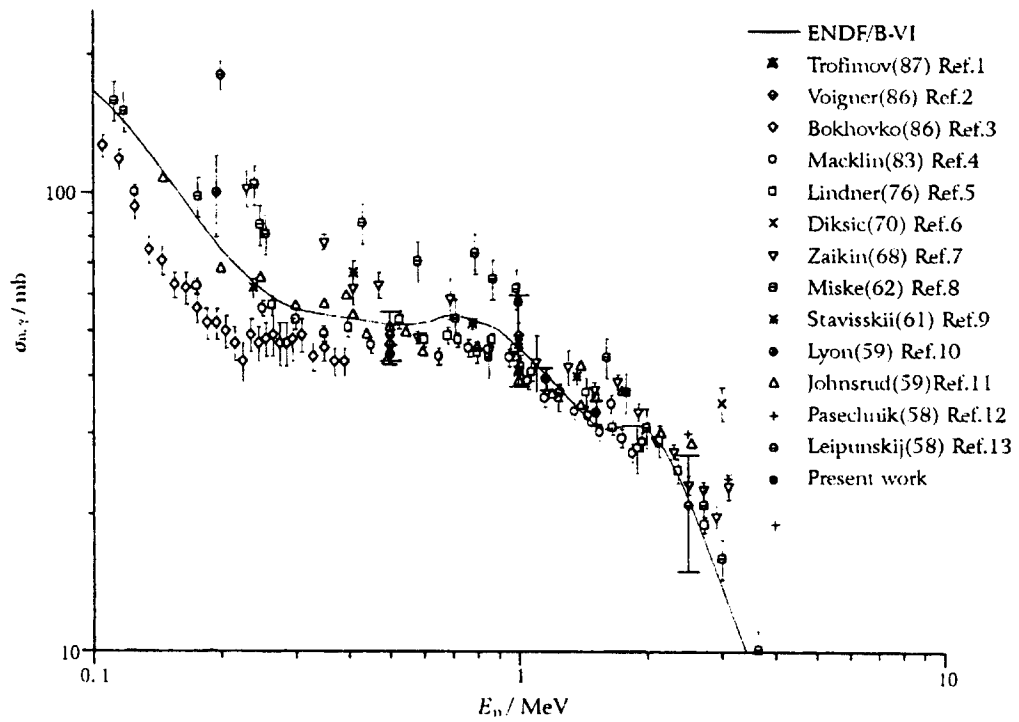


Fig.3 The cross section of  $^{186}\text{W}(N, \gamma)$  reaction

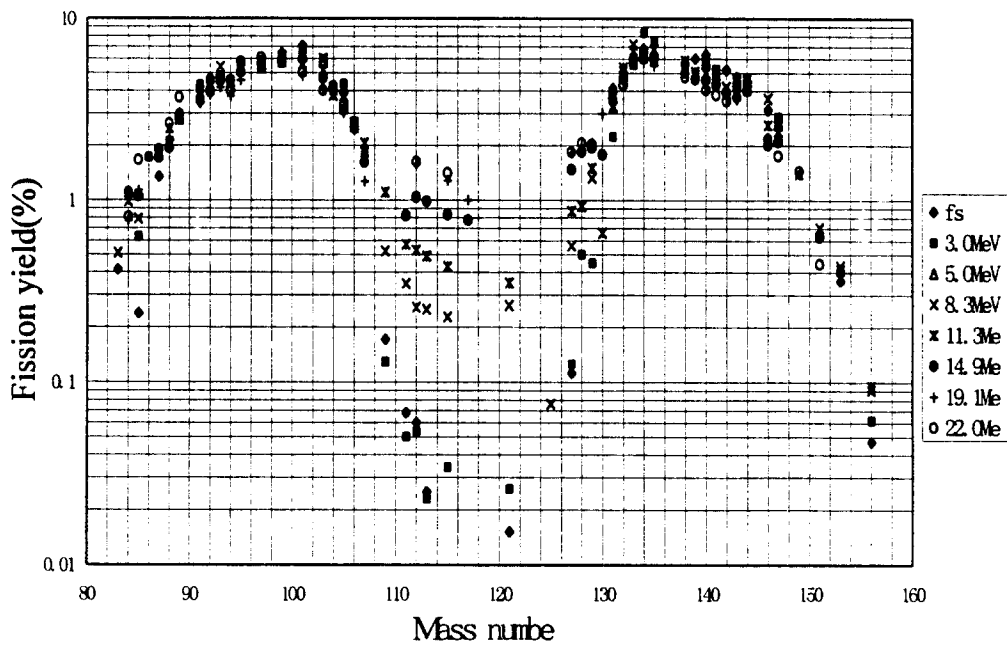


Fig.4 The mass distribution of product nuclides from for U-238 fission at 19.1 and 20.0 Me

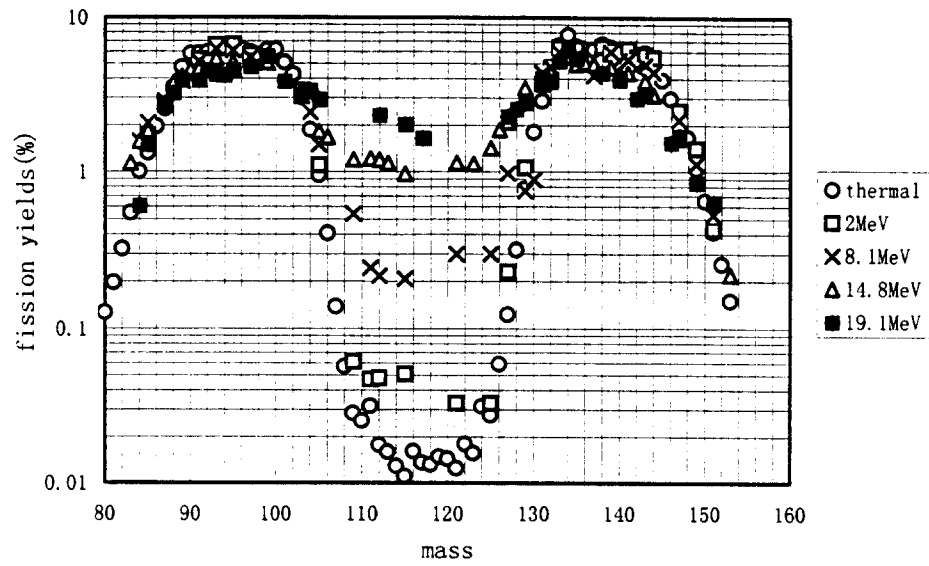


Fig. 5 The mass distribution of product nuclides from  $^{235}\text{U}$  fission at 19.1 MeV

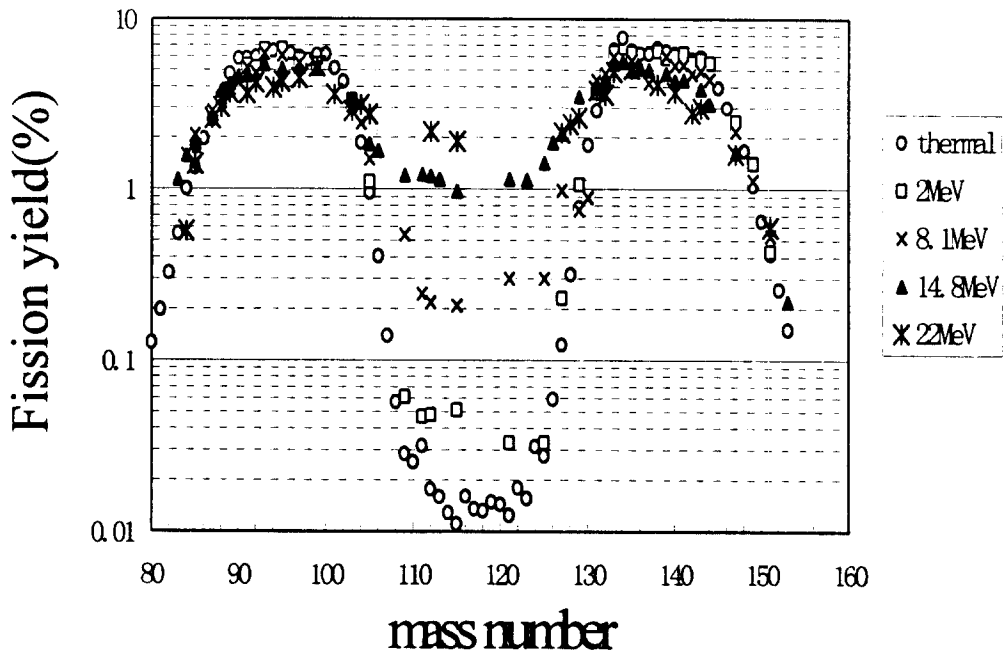


Fig. 6 The mass distribution of product nuclides from  $^{235}\text{U}$  fission at 22.0 MeV

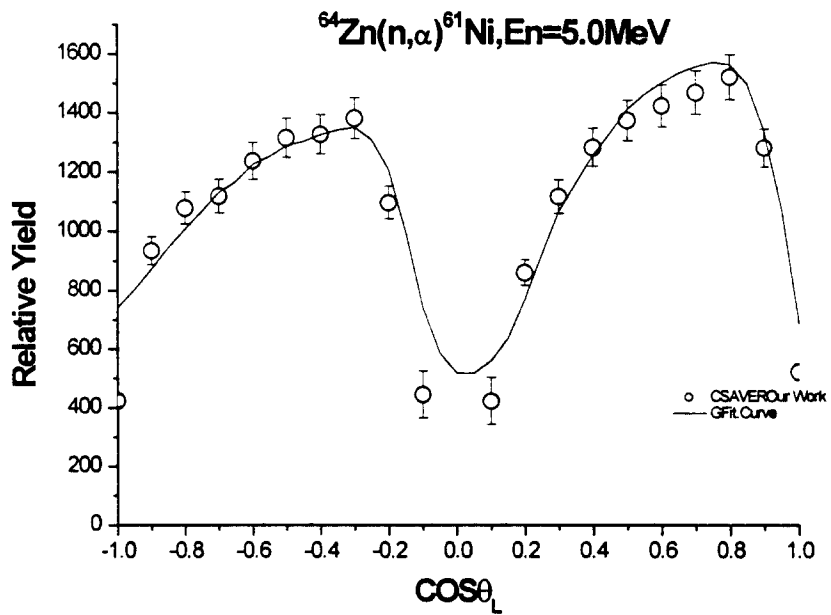


Fig. 7 Angular Distribution for  $^{64}\text{Zn}(n,\alpha)^{61}\text{Ni}$  reaction at  $5.0\pm 0.26$  MeV

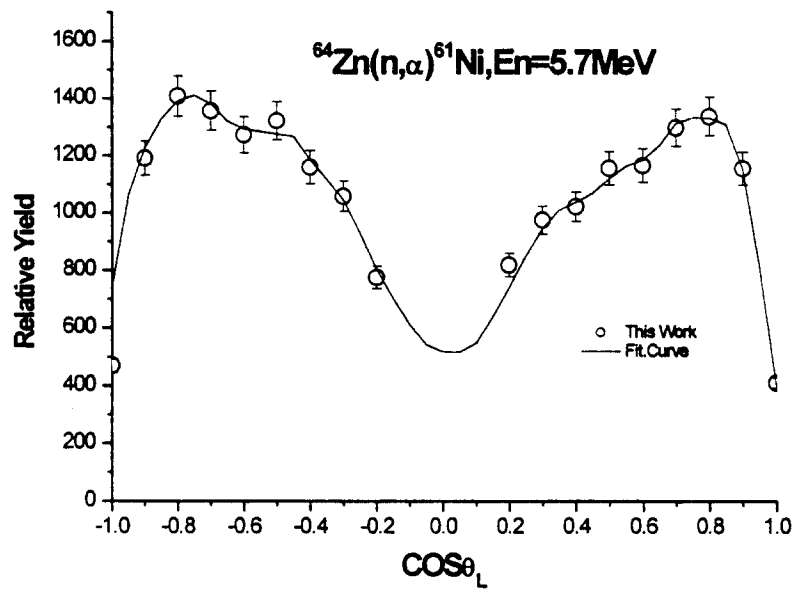


Fig. 8 Angular Distribution for  $^{64}\text{Zn}(n,\alpha)^{61}\text{Ni}$  reaction at  $5.7\pm 0.15$  MeV



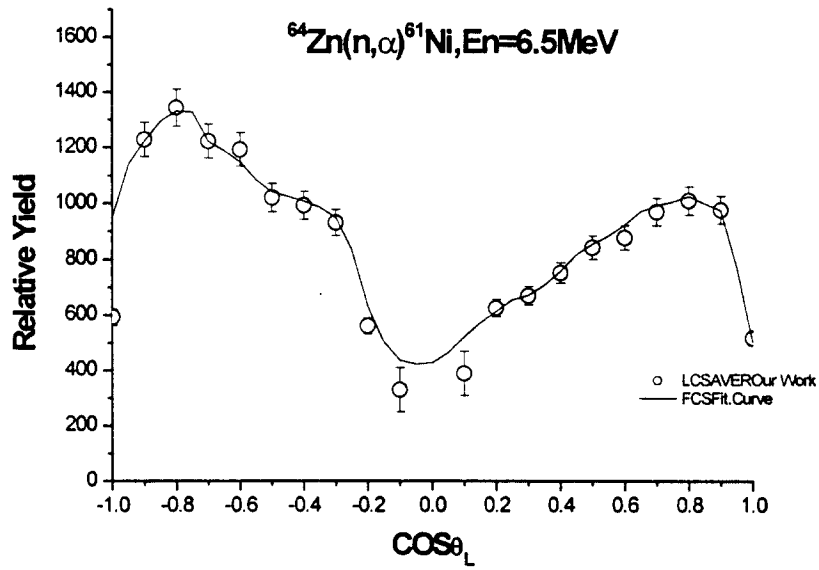


Fig. 9 Angular Distribution for  $^{64}\text{Zn}(n,\alpha)^{61}\text{Ni}$  reaction at  $6.5\pm 0.20$  MeV

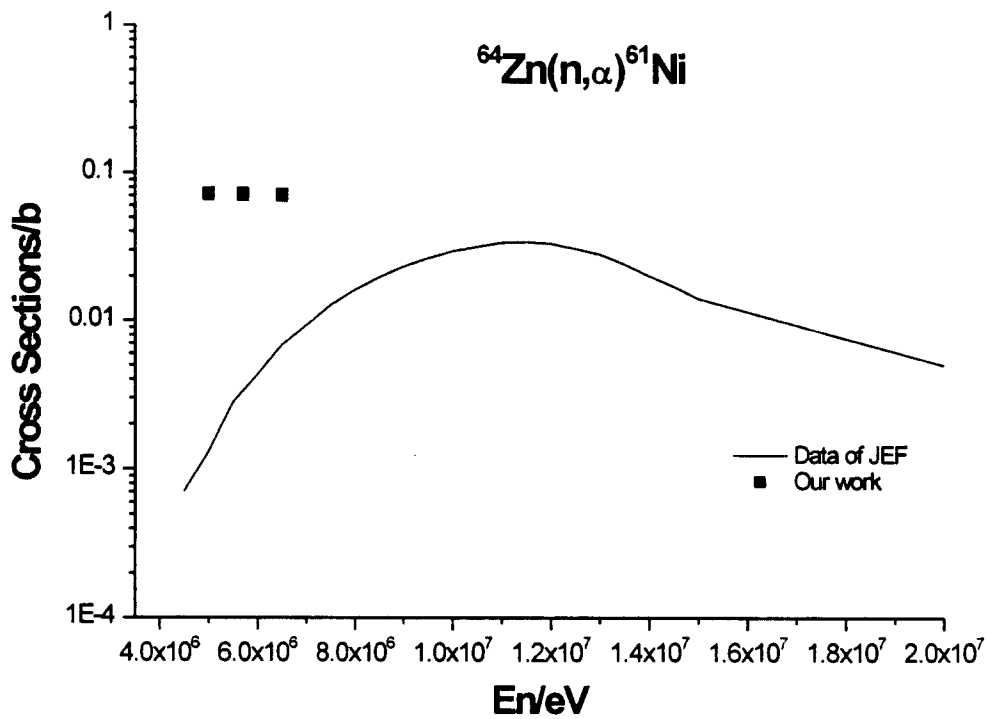


Fig. 10  $^{64}\text{Zn}(n,\alpha)^{61}\text{Ni}$  cross section compared with others

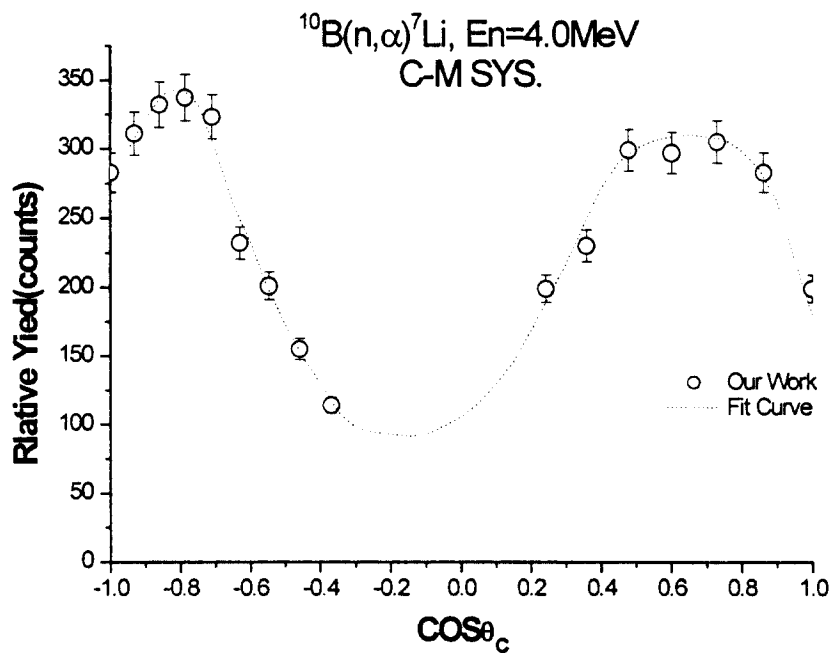


Fig. 11 Angular Distribution for  $^{10}\text{B}(n,\alpha)^7\text{Li}$  reaction at  $4.0\pm 0.20\text{ MeV}$

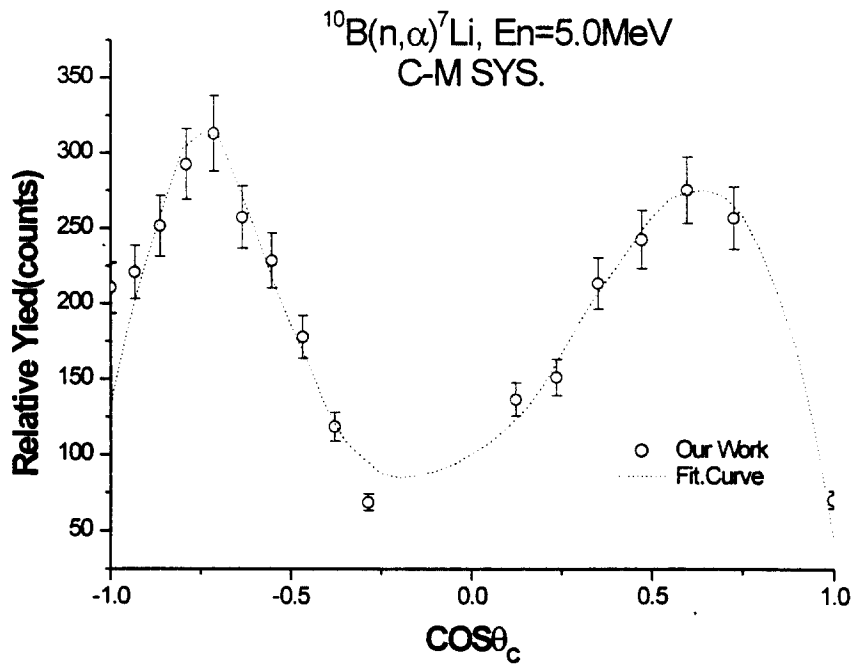


Fig. 12 Angular Distribution for  $^{10}\text{B}(n,\alpha)^7\text{Li}$  reaction at  $5.0\pm 0.26\text{ MeV}$

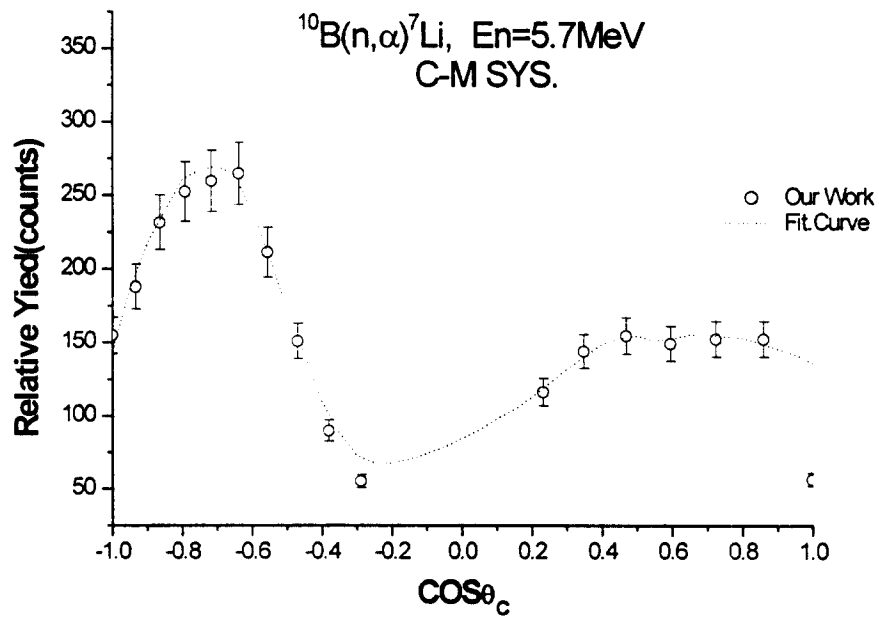


Fig. 13 Angular Distribution for  $^{10}\text{B}(n,\alpha)^7\text{Li}$  reaction at  $5.7\pm 0.15\text{ MeV}$

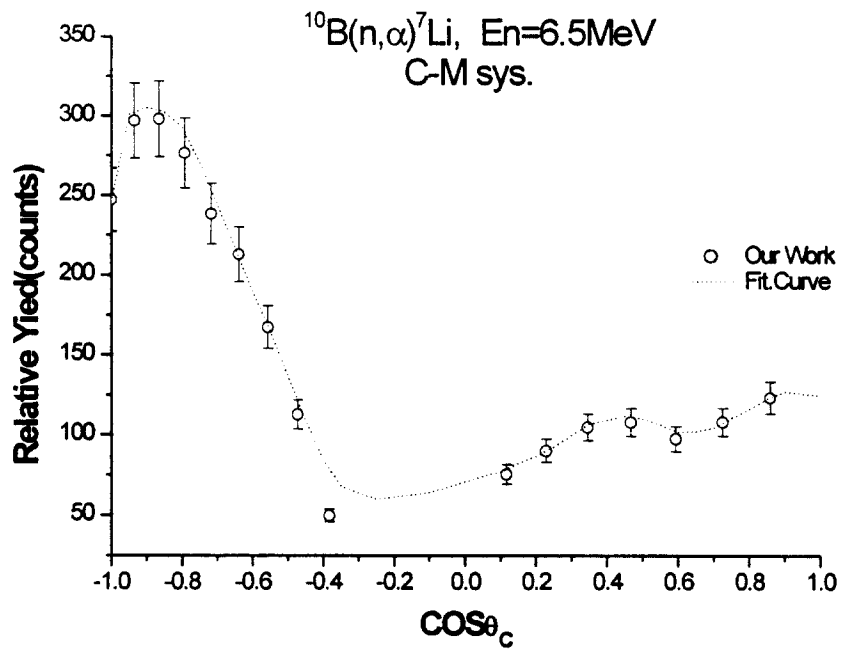


Fig. 14 Angular Distribution for  $^{10}\text{B}(n,\alpha)^7\text{Li}$  reaction at  $6.5\pm 0.20\text{ MeV}$

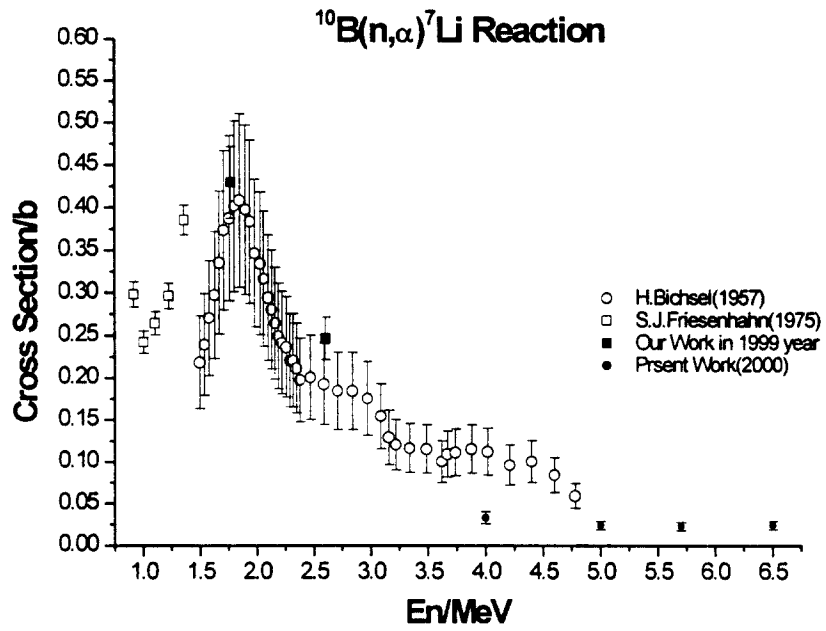


Fig. 15 The  $^{10}\text{B}(n,\alpha)^7\text{Li}$  cross section compared with other measurements